UNIVERSIDAD COMPLUTENSE DE MADRID

DEPARTAMENTO DE FÍSICA ATÓMICA, MOLECULAR Y NUCLEAR

PET - Positron Emission Tomography
An application of nuclear physics in diagnostic medicine

by

Ines Hörger

supervised by

Dr. **José Luis Contreras González**
Universidad Complutense Madrid
Madrid (Spain)

Dr. **José Manuel Udías Moinelo**
Universidad Complutense Madrid
Madrid (Spain)

Contents

Chapter 1

Medical Imaging - Introduction and Methods

1.1 What is medical imaging and why do we need it?

The human eye is able to see only the exterior part of a body. The mision of medical imaging is to obtain an image of the interior. The aim is an image of internal anatomical structure and functional properties. This information can then be used for diagnose but also for planning and monitoring the treatment of malignant disease.

The human body has very little natural emission of signals. It emits infrared photons and acoustic signals and produces electrical potentials. All these properties are used for analysis. The idea of how to achieve an image is to let the body (matter) interact with energy so that this energy is partially absorbed and partially passes through. Keeping this in mind different imaging methods based on different interactions of energy with biological structure can be thought of.

1.2 Methods and Techniques

X-Rays

The beginning of medical imaging can be set in 1895 when Roentgen discovered the x-rays, which still today are of major importance. Photons produced in an x-ray tube pass through tissue and are detected on the other side. The two-dimensional picture reflects the distribution of attenuating properties of the tissue. These photographs can reveal a detailed structure of the human skeletal system and are used for example to visualize broken bones. The disadvantages of this method are that it is not possible to distinguish between different types of

soft tissue (the attenuation coefficients of blood and muscle are very close) and that no depth information can be obtained. It is a non-tomographic technique as what we obtain is a projection of (a part of) the body.

Tomography / Computerized Tomography (CT) with x-rays

An image of a particular slice of the internal structure of the body is called a tomography. A first step might be the x-ray linear tomography. Here the x-ray tube and the film are moved simultaneously in opposite directions so that all points on a certain plane retain their locations on the film and points that are not on the plane are smeared or blurred. The result is a focused image of a particular slice but little contrast due to the smeared points on the film.
Nowadays very important is the Computed Tomography. A planar slice of the body is chosen and x-rays parallel to this slice pass through and are detected on the opposite. These data are collected from different directions so that a large number of one-dimensional density profiles is the result. By the help of a computer a two dimensional image of each slice is reconstructed containing depth information and high resolution.

Magnetic Resonance Tomography

Magnetic Resonance Tomography is another tomography method. It is not based on ionising radiation but on magnetic properties of certain nucleus (mainly protons) found or introduced in the body. Due to an enormous statical magnetic field a Zeeman δE splitting of the adjacent nuclear magnetic substates is obtained. A smaller high frequency magnetic field ($\nu = \delta E/h$) causes transitions between the substates. A third field, space dependent, correlates the resonance frequencies and positions inside the body. After switching of the HF field the excited states relax and emit radio-frequency power at the resonance frequency, which is detected. The obtained image therefore primarily reflects the proton spin density and the relaxation times and contains anatomical information. It is also possible to introduce tracers (substances marked with atoms or molecules having magnetic properties) into the body and to obtain functional information by their observation.

Techniques not based on nuclear medicine

Other techniques which are not based on nuclear medicine and which I will only mention here are Ultrasound, Infrared Imaging, Electrical Impulses or Diaphanography.

Radioisotope imaging

Radioisotope imaging is in contrary to the above methods, which are mainly anatomical, a functional method. It consists of introducing a substance marked with a radioisotope into the patients body. This substance should concentrate in the region of the body or the organ which wants to be analyzed giving functional information (for example about metabolism). Two main methods are used, the Single Photon Emission Tomography (SPECT), where the tracer emits *gamma*-rays and the Positron Emission Tomography (PET) which works with positron emitting substances and will be our main concern in this work.[1]

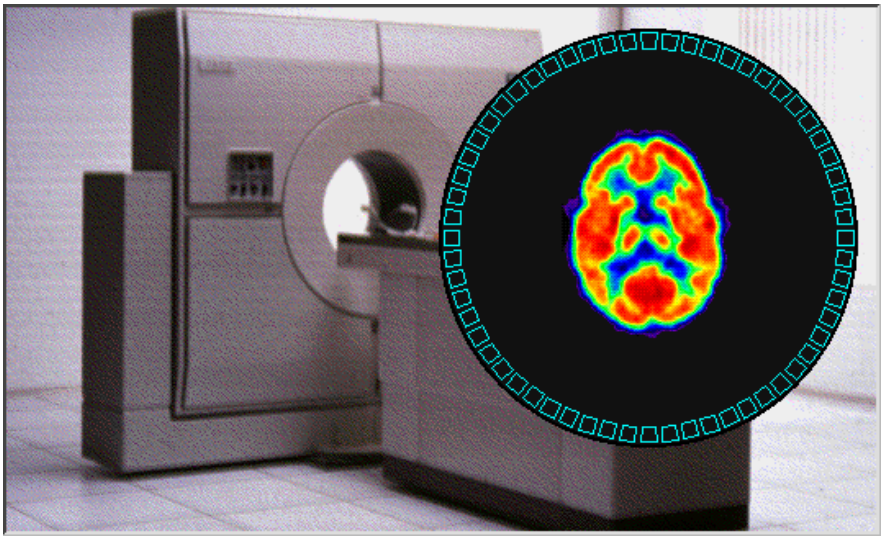

Figure 1.1: PET scanner and reconstructed image [2]

Chapter 2

Functional Imaging and Tracers

SPECT and PET are based on the detection of the distribution of radiopharmaceuticals in the body yielding a functional image. A functional image reflects dynamic physiological processes in the body. It is possible to study a great number of biological functions such as organ motion (heart, blood flow), excretory functions (kidneys, liver) or metabolic processes. The two major fields of interest are the study of physiological function of tissue or an organ and the localization of disease like for example a tumor. A radiopharmaceutical consists of a radioisotope, which is bound to a specific molecule. To obtain best possible results and at the same time cause the least possible effects on the body, the radiopharmaceutical should have certain properties. The labeled molecules are also called tracers. Since the aim is to concentrate the tracer in the part of the body or the organ that is wanted to be analyzed specific biological and chemical behavior of the tracer is necessary. As biochemical molecules that naturally appear in the organism all have low Z $(C, H, O, ...)$, it would be very useful to have radioisotopes with low Z as well.

Radioisotopes in SPECT

The problem of SPECT is that within the artificially created radioisotopes of low Z there aren't any γ-emitters with reasonably half life so that the challenge here is to find radio-pharmaceuticals which are labeled with high Z radionuclides but show a behavior similar to natural biological molecules. The characteristics of radionuclides used in SPECT should be:

- decay via photon emission and absence of particle emission
- a half-life suitable to the length of study
- the photon energy should be high enough to penetrate tissue but low enough to be efficiently detected with a γ-camera

The radionuclide used in 90% of all nuclear medicine studies is the $^{99}Tc^m$ which emits $140keV$ γ-rays via isomeric transition. Its half-life is $6h$. Other radioisotopes commonly used include ^{123}I,^{111}I,^{67}Ga,^{211}TI and $^{81}Kr^m$.

Radioisotopes in PET

For PET diagnostic the radioisotopes are positron emitters and can be easily found within the lighter elements. Radionuclides used for PET should decay via positron emission and have a half-life suitable to the length of study.

Radionuclide	$T_{1/2}$
^{11}C	20,4 min
^{15}O	2,07 min
^{13}N	9,96 min
^{18}F	109,7 min
^{68}Ga	67,8 min
^{82}Rb	1,26 min

Table 2.1: Most frequently used β^+-emitters and their half-lives

These radionuclides are usually produced by charged-particle bombardment, in this case often with protons (H^+). The stable isotopes are bombarded by a proton beam with energy smaller than 12 MeV. The protons are produced by small cyclotrons. Often used are accelerators for negative ions (H^-) that are later transformed into protons by ion stripping. Reactions for the production of radioisotopes are for example:

$$
\begin{aligned}
{}^1_1H_+ + {}^{14}_7N &\longrightarrow {}^{11}_6C + {}^4_2He^{2+} + e^- \\
{}^1_1H_+ + {}^{13}_6C &\longrightarrow {}^{13}_7N + n + e^+ \\
{}^1_1H_+ + {}^{15}_7N &\longrightarrow {}^{15}_8O + n + e^+ \\
{}^1_1H_+ + {}^{18}_8O &\longrightarrow {}^{18}_9F + n + e^+
\end{aligned}
$$

Because of the small half-lives of the radioisotopes the cyclotron and the chemical procedure for the production and control of the labeled molecules should be situated near the center of analysis, which limits the availability to clinical nuclear medicine. An exception is ^{18}F, having a half-life that allows a regional distribution. A good radiopharmaceutical is supposed to be easily synthesized and it must be free of any contamination.

Almost all biological molecules can be labeled with positron emitters without changing the biological and chemical properties. The distribution of the tracer in the body depends on various factors like the molecule size and its shape, the degree and strength of protein binding in tissue and blood, lipid solubility or specific cell mechanisms.

As an example I will mention the analysis of the brain. Although a great number of analysis are possible by conventional nuclear medicine, PET provides unique possibilities like quantitative functional information that can distinguish between normal brain activity and changes in metabolism and function caused by cerebral disease.

<table>
<tr><th>Radionuclide</th><th>Tracer</th><th>Analyzed Function</th><th>Information</th></tr>
<tr><td>^{15}O</td><td></td><td>oxygen-extraction efficiency of normal and abnormal brain tissue</td><td>aerobic / anaerobic</td></tr>
<tr><td rowspan="3">^{18}F</td><td rowspan="3">FDG (Fluorodeoxyglucose)</td><td>mimic glucose metabolism rates of the brain</td><td>metabolic function</td></tr>
<tr><td colspan="2">localization of functioning during visual processes like reading or viewing (FDG is metabolised similar to glucose)</td></tr>
<tr><td colspan="2">information about cerebral defects</td></tr>
<tr><td>^{68}Ga</td><td>EDTA</td><td>blood-brain barrier</td><td rowspan="3">abnormalities indicate tumors</td></tr>
<tr><td>^{11}C</td><td>methionine</td><td>study of protein synthesis</td></tr>
<tr><td></td><td>glucose</td><td>glucose metabolism</td></tr>
<tr><td>^{11}C</td><td rowspan="2">receptor-binding tracers</td><td colspan="2" rowspan="2">localization of

neurological function</td></tr>
<tr><td>^{18}F</td></tr>
</table>

Table 2.2: Different radioisotopes and their application in brain imaging

By far the most important tracer used in PET is FDG. Due to its long half-life this radiopharmaceutical can be transported from the center of production to centers only equipped with a PET tomograph. It is easily and rapidly synthesized, has unique metabolic properties (similar to those of glucose) and a great range of applications. [3][4]

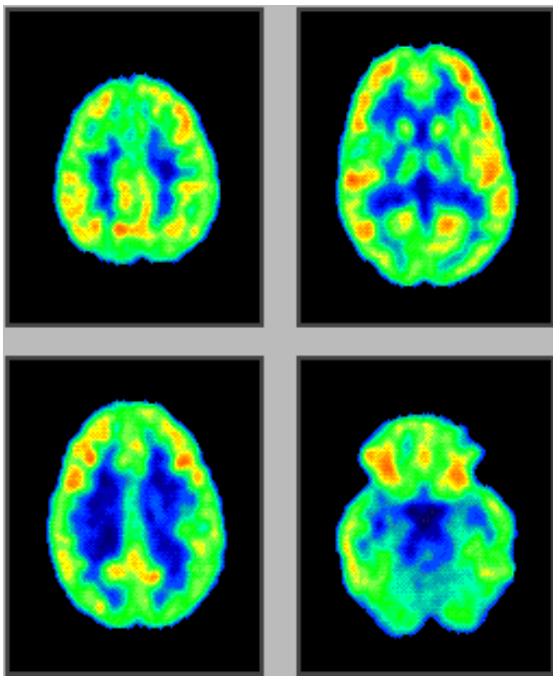

Figure 2.1: Different slices of a brain at rest [5]

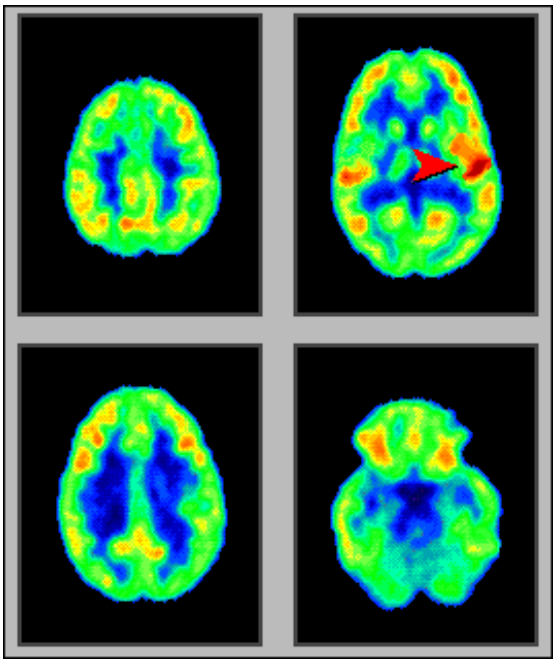

Figure 2.2: Effects in the brain because of listening to music. Activation of the right hemisphere [6]

Chapter 3

Detection of γ-rays, the problem of creating images

The detection of the γ-ray is a difficult problem on the way of creating an image. There are no "lenses" for γ-rays. They are uncharged particles so that electric or magnetic fields cannot take influence on their trajectory. The wavelengths of γ-rays are much smaller than the atom diameter ($2,4 * 10^{-12}m$ for $511keV$ photons) so that focusing isn't possible with any material.
In order to be detected γ-rays have to interact in some way with matter. Although there are different types of interactions of γ-rays with matter, they always interact with the detector electrons. In contrary to α- or β- rays the cross section for interaction is (depending on the detector material and the photon energy) relatively low and the ranges of photons are much higher than the ranges of αs and βs. γ-rays transmit part of their energy or their total energy to electrons. These electrons then are collected. Usually the detection of a photon is an "all or nothing" process. Or they are detected leaving all their energy in the detector or they pass through (leaving maybe part of their energy but not enough to be detected).

There are three main processes in which γ-rays interact with matter, the photo electric effect, the Compton effect and the pair production. As the latter one is only possible for γ energies above twice the electron rest energy we will only discuss photo electric and Compton effect.

Photo electric effect

A photon is completely absorbed by an atom and a photoelectron is released. The energy of the photoelectron is the γ-energy minus the binding energy of the electron in the atom ($T_e = E_\gamma - E_B$). A small part of the initial γ-energy also goes to the atom which in order to guarantee momentum conservation will receive a recoil. The cross section of the photo electric effect is strongly dependent on

the atomic number Z of the material and the initial energy of the photon E_γ.

$$\sigma = \frac{16\sqrt{(2)}\pi}{3}\alpha^8 Z^5 \left[\frac{m_e c^2}{\hbar\omega}\right]^{1/2} (a_0)^2$$

This calculation is made for a hydrogen atom and is approximately valid for inner ejection of an electron of an inner shell. a_0 is the Bohr radius for an hydrogen atom and $\alpha^2 = \frac{e^2}{4\pi\epsilon_0 a_0 mc^2}$. So in general the cross section decreases with increasing photon energy. But every time the photon energy reaches the amount of the binding energy of a particular electronic shell we notice a jump in the cross section.

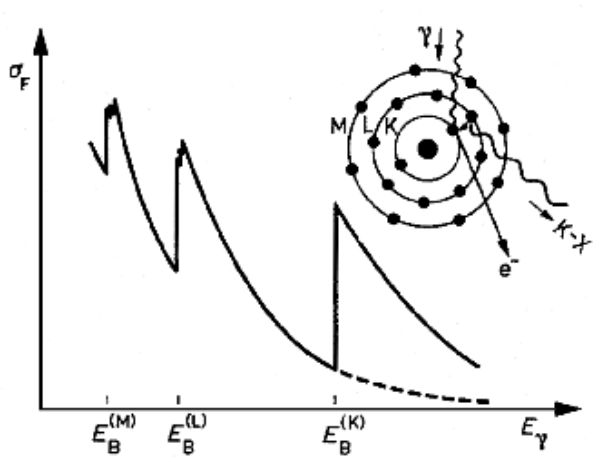

Figure 3.1: Cross section of photo electric effect as a function of the photon energy [7]

Compton-effect

The Compton effect is a scattering process between a photon and an electron. The electron can be considered as practically free often being an outer shell atomic electron. According to energy and momentum conservation laws, the photon suffer an energy loss and changes its direction, the electron receives the lost energy.

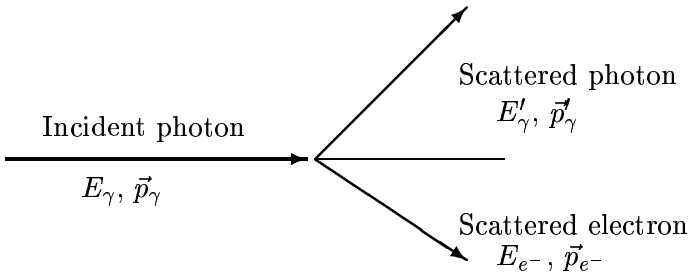

The probability of this process can be determined through quantum mechanical calculations and the result is the Klein-Nishima-formula:

$$\sigma_c = \frac{\pi r_0^2}{\alpha}\left[(1-\frac{2(\alpha+1)}{\alpha^2})ln(2\alpha+1)+\frac{1}{2}+\frac{4}{\alpha}-\frac{1}{2(2\alpha+1)^2}\right]$$

with $\alpha = \frac{E_\gamma}{mc^2}$ and $r_0 = \frac{e^2}{4\pi\epsilon_0 mc^2}$. σ_c refers to the cross section per electron, so that the cross section in a certain material would be:

$$\sigma = \sigma_c NZ$$

where Z is the atomic number and N the density of atoms. The Compton cross section decreases with increasing γ-energy and increases (although only linearly) with increasing atomic number.

A comparison between the probabilities for photo electric effect and Compton effect shows, that photo electric effect dominates for low γ-energies and high Z.

One problem on the way of forming an image is that although we are able to detect the photon it results almost impossible to determine its momentum - or the direction from where it proceeds. Although it was possible to determine the momentum of the released electrons a calculation back to the photon momentum remains difficult. Attempts to localize the proceeding of the photon are made in Compton-PET where the electron and the scattered photon are detected simultaneously and so an estimation of the initial γ-momentum is possible. [8]

Chapter 4

Physical basics of PET

The radioisotopes introduced into the body are, in case of PET, positron emitters but what finally is detected are photons. What happens between the emission of a proton and its detection as photon? Positrons are emitted with different energies (see next chapter). Because of scattering with surrounding molecules they loose kinetic energy until they reach thermal energy. These thermal photons then annihilate with electrons into photons.

This process of course has to conserve total momentum and energy of proton and electron. The following calculation shows, that the conservation law couldn't be completed by annihilation into a single photon. Relativistic energy and momentum of the electron-positron pair are $E = \frac{mc^2}{\sqrt{1-(v/c)^2}}$ and $p = \frac{mv}{\sqrt{1-(v/c)^2}}$. The photon would have to carry energy and momentum of the electron-positron pair. Its energy-momentum relation $E = pc$ would give $\frac{mv}{\sqrt{1-(v/c)^2}} = \frac{mc}{\sqrt{1-(v/c)^2}} \Longrightarrow v = c$, an equation forbidden by relativistic dynamics. The most frequent and important case is the annihilation into two γ-particles, but also the annihilation into three or more photons is possible.

The cross section for the annihilation of an e^- - e^+ pair is:

$$< \sigma >= \pi r_o^2 c/v$$

v is the (small) relative velocity of the e^- - e^+ pair, c the velocity of light and r_0 the radius of the electron. $< \sigma >$ refers to the average over the two possible mutual directions of the spins ($\uparrow\uparrow$ and $\uparrow\downarrow$). This equation is valid for $(e^2/\hbar c)mc^2 \ll T \ll mc^2$ with T being the relative kinetic energy of the e^- - e^+ pair. For higher kinetic energies relativistic dynamics would have to be used in the calculation.

As the cross section is given per electron, the probability of annihilation will

also depend on the electron density in the material. The distance the positron travels before annihilation is called its range. The range depends on its maximum energy (and therefore on the nucleon where it proceeds from) and on the electron density of the tissue. Mean values for ranges lie between $0,35mm$ (for ^{18}F) and $1,1mm$ (for ^{15}O or ^{68}Ga), maximum ranges between $2,4mm$ (for ^{18}F) and $9,1mm$ (for ^{68}Ga) .

A bound state between an electron and a positron is called positronium. In its ground state it appears in the singlet and triplet S state with orbital angular momentum 0.

Singlet	Triplet
$^3S_1$	$^1S_0$
$\uparrow\uparrow$	$\uparrow\downarrow$
annihilates	annihilates
into 3 γs	into 2 γs

Due to angular momentum conservation only for the singlet state it is possible to annihilate into 2 γs. These 2 γs spread out collinear in opposite directions. Measuring the polarisation we find γ_1 linear polarised in a given direction (left circular polarised) and γ_2 linear polarised in direction perpendicular to that of γ_1 (right circular polarised). For the triplet state the annihilation into 2 γs is not possible and it will annihilate into 3 γs. Having another look at the cross section for the annihilation into 2 photons we find a difference between singlet and triplet state:

$$
\begin{aligned}
{}^3\sigma_{2\gamma} = 0 \qquad & {}^1\sigma_{2\gamma} = 4\pi r_0^2 c/v \\
<\sigma_{2\gamma}> \;=\; & \left(\frac{3}{4}\right)^{trip}\sigma_{2\gamma} + \left(\frac{1}{4}\right)^{sing}\sigma_{2\gamma}
\end{aligned}
$$

To compare the probabilities for annihilation into 2 or 3 photons we calculate the mean lifetime of the electron positron system for the two processes.

$$\frac{1}{\tau} \;=\; \sigma_{2\gamma}\rho v$$

with τ being the mean life time and ρ the electron density which in the bound case will be the density of electrons at the positron position $|\psi(0)|^2$.

$$\frac{1}{\tau} \;=\; {}^1\sigma_{2\gamma} v |\psi(0)|^2$$

$$\begin{aligned} &= 4\pi r_0^2 c \frac{1}{\pi} \left(\frac{1}{2na_0}\right)^3 \\ &= \frac{1}{2}\left(\frac{e^2}{\hbar c}\right)^5 \frac{mc^2}{\hbar}\frac{1}{n^3} \\ &= \frac{1}{1,24 \cdot 10^{-10} n^3}\frac{1}{s} \end{aligned}$$

with a_0 being the Bohr radius and n the total quantum number of the orbit so that the mean life time grows with n^3 and the annihilation is indeed most probable for the ground state. Doing the calculation for the triplet state shows that its mean lifetime is about 1115 times longer. The probability of annihilation into 3 photons compared to the probability of annihilation into 2 photons is therefore:

$$\frac{\left(\frac{3}{4}\right)^{trip}\sigma_{3\gamma}}{\left(\frac{1}{4}\right)^{sing}\sigma_{2\gamma}} = \frac{3}{1115} = \frac{1}{372}$$

As the probability for annihilation into 3 photons is very small, we will neglect it and only consider the annihilation into 2 photons. [9]

Chapter 5

Theory of β^+-decay

A process which converts a proton into a neutron or a neutron into a proton is called β-decay. Three different processes exist:

$$\begin{array}{ll} n \longrightarrow p + e^- + \bar{\nu} & \beta^- \text{ decay} \\ p \longrightarrow n + e^+ + \nu & \beta^+ \text{ decay} \\ p + e^- \longrightarrow n + \nu & \text{electron capture } (\epsilon) \end{array}$$

The number of nucleons in the nucleus remains constant and the atomic number increases by one (β^--decay) or decreases by one (β^+-decay). The existence of the neutrino (ν) was suggested by Pauli in 1931 in order to fulfill energy and momentum conservation and the existence of this almost massless particle has been proved in experiments.

Energy release

The energy distribution of the β-particles is continuous and goes from zero to an upper limit equal to the energy difference between initial and final state. Q, the value of the difference of initial and final nuclear mass energies is (for the $\beta+$ decay) calculated as follows:

$$Q_{\beta^+} = [m_N({}^A_Z X) - m_N({}^A_{Z-1} X') - m_e]c^2$$

As it is easier to calculate with the tabulated atomic masses, we will transform the equation:

$$Q_{\beta^+} = m({}^A_Z X)c^2 - Zm_e c^2 + \sum_{i=1}^{Z} B_i - m({}^A_{Z-1} X') + (Z-1)m_e c^2 - \sum_{i=1}^{Z-1} B_i - m_e c^2$$

$$\begin{aligned} &= [m(^A_Z X) - m(^A_{Z-1} X') - 2m_e]c^2 \\ &= T_e + E_\nu \end{aligned}$$

The energy that is gained in the process is shared between the electron and the neutrino. A negligible small part also goes to the nucleon as recoil energy. As the neutrino is almost massless it can be treated in the ultrarelativistic limit and its mass can be neglected in the energy calculation. The last equation shows, that depending on the neutrino energy, the β^+ will have an energy between 0 and Q_{β^+}. The equation also shows, that to make the process possible, the mass difference between initial and final nucleon must be at least twice the electron mass. The same calculation for electron capture (combining the same initial and final nucleon as the β^+ decay) shows that for this process the two-electron-mass energy difference is not necessary:

$$Q_\epsilon = [m(^A_Z X) - m(^A_{Z-1} X')]c^2$$

For each nucleon that may suffer β^+ decay also electron capture is energetically allowed and can therefore be considered as a concurrence process. Later on we will see, that for the nuclei used in PET the ratios of electron capture are much smaller than the ratios for β^+-decay.

Calculations based on the Fermi theory of β-decay give the energy distribution of the β-particles in the "allowed approximation" (see following paragraph).

$$N(T_e) = \frac{C}{c^5}(T_e^2 + 2T_e m_e c^2)^{1/2}(Q - T_e)^2(T_e + m_e c^2)$$

Angular momentum and parity selection rules

The probability for β-decay depends on the angular momentum and parity of the initial and final nucleon state. The decays are divided into allowed and first-, second-, third-, ... forbidden decays.

Allowed decays

In the calculations for the allowed decays an approximation supposing the positron and the neutrino to have orbital angular momentum $l = 0$. The angular momentum they carry proceeds exclusively from their spins and can have the values $S = 0$ (antiparallel spins) or $S = 1$ (parallel spins). As the angular momentum

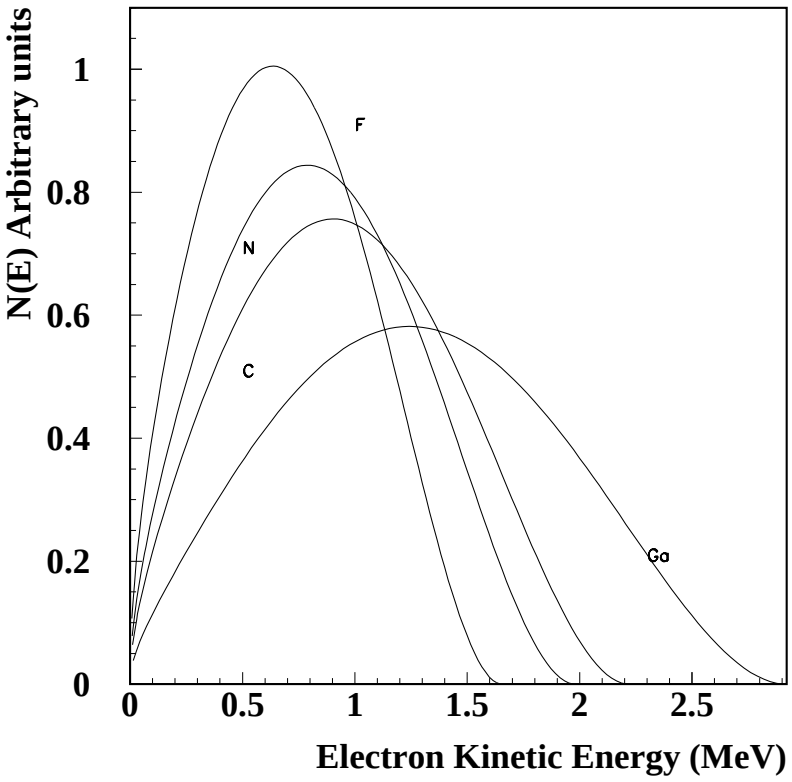

Figure 5.1: Energy distribution for ${}^{11}_{6}C$, ${}^{13}_{7}N$, ${}^{18}_{9}$, ${}^{68}_{31}Ga$

must be conserved in the transition the difference between the spins of the initial and the final nucleon states must be $\Delta J = 0$ or $\Delta J = 1$.
The parity of the positron and the neutrino is associated to the orbital angular momentum l ($\pi = (-1)^l$) and in the allowed approximation ($l = 0$) $\pi = 1$. So the initial and final nucleon states must have the same parity.
We therefore have the following selection rules for allowed decays:

$$\Delta J = 0, 1 \qquad \Delta\pi = no$$

Forbidden decays

"Forbidden" decays are called like this because their probability is usually much smaller than the probability for allowed decays. For first-forbidden decays we assume the positron and the neutrino to have angular momentum $l = 1$ and the

same conclusions as made for allowed decays give the following selection rules:

$$\Delta J = 0, 1, 2 \qquad \Delta\pi = yes$$

In this way we can go on for second-, third-, ... forbidden decays.
As the decay probability decreases with increasing forbiddingness, the half-lives of the nuclei grow. [10]

Examples of nuclei used in PET

$^{11}_{6}C$

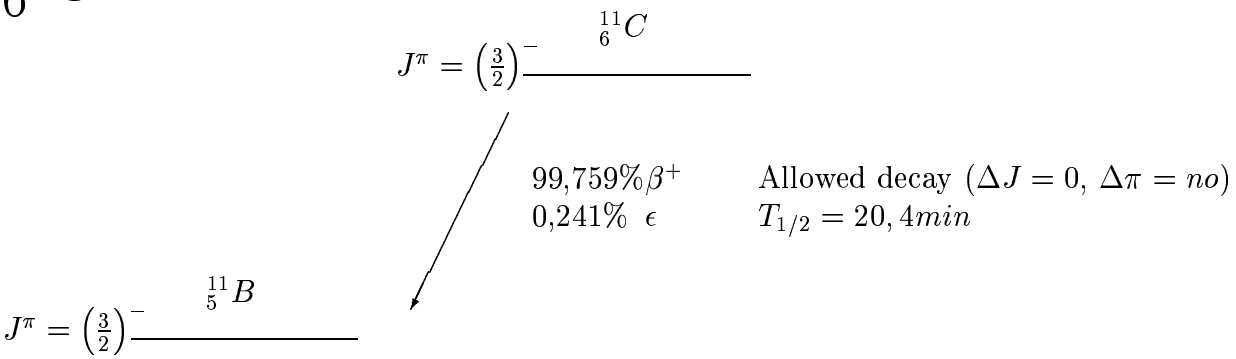

$^{13}_{7}N$

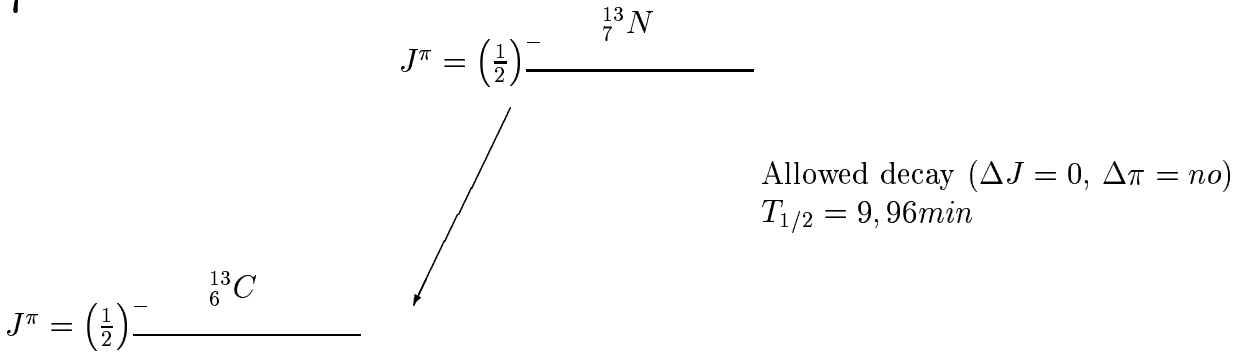

$^{15}_{8}O$

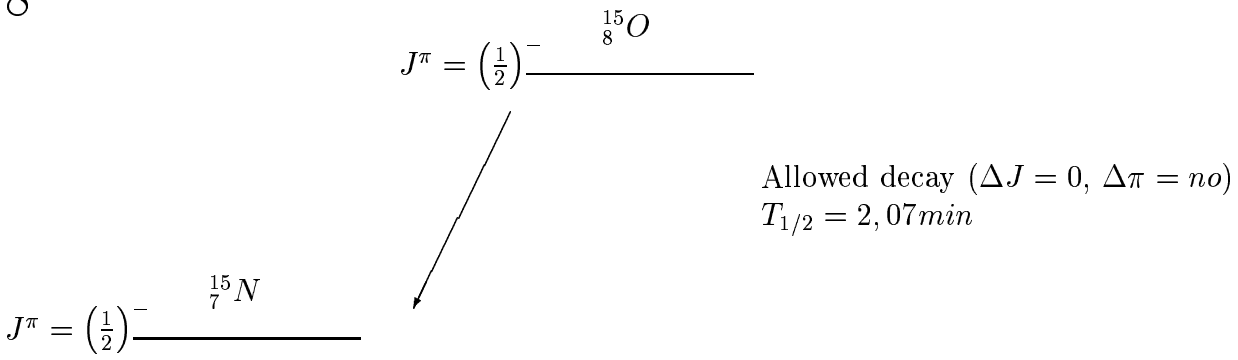
$^{15}_{8}O$
$J^\pi = \left(\frac{1}{2}\right)^-$
Allowed decay ($\Delta J = 0$, $\Delta\pi = no$)
$T_{1/2} = 2,07min$
$^{15}_{7}N$
$J^\pi = \left(\frac{1}{2}\right)^-$

$^{18}_{9}F$

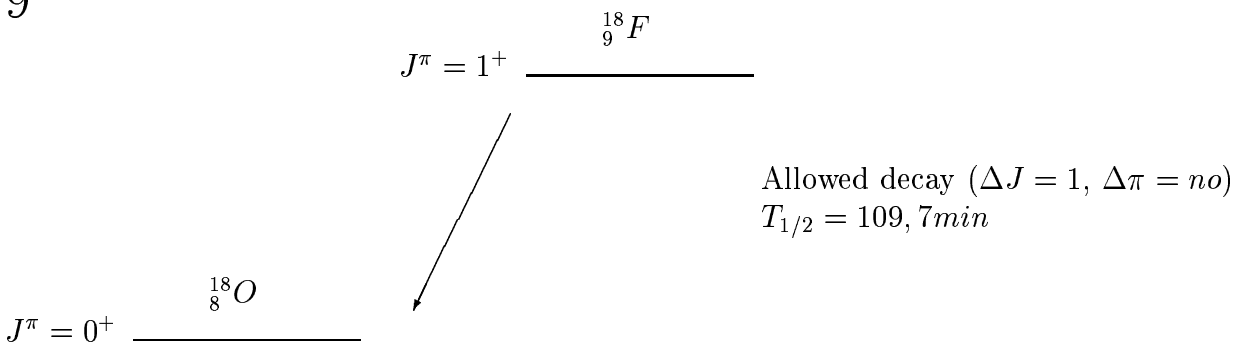
$^{18}_{9}F$
$J^\pi = 1^+$
Allowed decay ($\Delta J = 1$, $\Delta\pi = no$)
$T_{1/2} = 109,7min$
$^{18}_{8}O$
$J^\pi = 0^+$

Chapter 6

Scintillation Detectors and Photomultipliers

To detect the γ-rays produced by the annihilation of the positrons with electrons we use a system consisting of a scintillation detector and a photomultiplier. Scintiallation detectors are made up of certain materials that have one property in common: they emit a small flash of light when they are struck by radiation or particles. The photomultiplier then converts the photons into a small current of electrons, which are further amplified by an electronmultiplier system. The electrical pulses are analyzed by an electronics system. I will now first talk about the scintillation detectors and the crystals used in PET, afterwards about the photomultiplier then about the connection between the two elements and finally about how the current is transformed into a final signal.

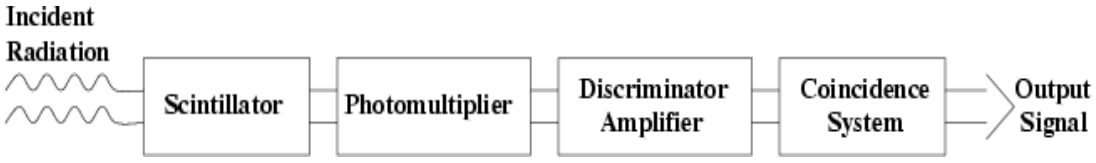

Figure 6.1: Principle setup of the detection system

6.1 Scintillation Detectors and Characteristics of the utilized Crystals

The detection system consists of a scintillating material that is optically coupled to a photomultiplier system. Radiation excites the atoms and molecules of the scintillator and causes them to emit light. The reemission of light may occur almost immediately (after about $10^{-8}s$ which is the decay time for atomic transitions) and is then called fluorescence or (if the excited state is metastable) it may

occur delayed and is then called phosphorescence or afterglow. The evolution of the process may be described as an exponential decay with two components, the fast and the slow component:

$$N = Aexp\left(\frac{-t}{\tau_f}\right) + Bexp\left(\frac{-t}{\tau_s}\right)$$

N is the number of photons emitted at time t, τ_f and τ_s are the fast and the slow decay constant. A and B depend on the material, usually dominating the fast component. In general a good detector scintillator should satisfy the following requirements:

- high efficiency for conversion of exciting energy to fluorescent radiation
- transparency to its fluorescent radiation so as to allow transmission of the light
- emission in a spectral range consistent with the spectral response of existing photomulitpliers
- short decay constant τ

Various types of scintillator materials are in use (organic crystals and liquids, plastics, inorganic crystals, gases and glasses) having different properties and being chosen according to the radiation or particles to be analyzed. The materials used for PET are inorganic crystals. Due to their relatively high Z the cross section for photo electric effect ($\propto Z^5$) is quite high compared to the cross section for Compton scattering ($\propto Z$). This is important because by photo electric effect the photon leaves all of its energy in the detector whereas by Compton scattering only part of the energy is transmitted to an electron and the scattered γ - if it doesn't suffer another interaction - may escape having deposited only part of its energy.

Inorganic scintillation crystals

- $Na(TI)$
  $Na(TI)$ was the material used for about 50 years in nuclear medicine, also in the first PET systems. Its most positive property is its high light emission but various other characteristics could be improved in order to fulfill the requirements of a good PET scintillator crystal. The Compton/photo ratio for $511keV$ photons is close to 5. To obtain an intrinsic sensitivity of 70% a crystal length close to $4cm$ is needed. The cross section of the crystals used in PET systems was about $2cm^2$. Making the cross section smaller to improve resolution the loss of Compton photons decreases its

Name	Density (gcm^{-1})	Effective atomic number	Radiation length (cm)	Hydros-copic	Relative Decay time (ns)	Light emission
$NaI(TI)$	3,67	51	2,56	Yes	230	100
BGO	7,13	75	1,12	No	300	15
GSO	6,7	59	1,38	No	60	25
LSO	7,4	66	1,14	No	40	75
CsF	4,64	52	2,00	Yes	5/0,6/0,8	5
BaF_2	4,88		1,9	slightly	630/0,6-0,8	16/3

Table 6.1: Most frequently used scintillator crystals in PET-systems and some of their characteristics

sensitivity. Another problem is that $Na(TI)$ is hygroscopic and hence has to be encapsulated. The research for more suitable materials during the last years has brought up a variety of new inorganic crystals.

- *BGO*
  Due to its high density and its high atomic number, BGO has a much shorter radiation length than $Na(TI)$ and a detector efficiency of 70% can be obtained with only $15mm$ long crystals. As the Compton/photo ratio is close to 1 the crystal cross section can be kept small (about $0,2cm^2$) and the resolution is therefore quite high. Another advantage is that BGO is not hygroscopic. But also BGO has problems and is not a perfect PET material: it is a quite slow crystal and has little light output. Its energy resolution lies between 23 and 25 %. Despite this, BGO has been used for 15 years in $2D$-PET systems and optimized for this kind of acquisition.

- *GSO* and *LSO*
  GSO and LSO are two new materials which are used or will be used in $3D$-PET systems. These new developments show various advantages for the patient: the sensitivity grows about 4 or 5 times, therefore the quantity of the radioisotope incorporated and hence the dosimetric exposition of the patient will decrease to between the half and one third and the necessary time of analysis for the whole body will decrease by a factor two. Comparing the two materials shows, that -although both have a good decay time- LSO is a bit faster, its light emission is considerably higher and the 70% detector efficiency is reached with $4mm$ long crystals, by GSO with $11mm$ long crystals. The advantage which has GSO is its higher energy resolution (14%, LSO18%). The production of GSO is easier and cheaper than the production of LSO.

- CsF and BaF_2
  CsF and BaF_2 have the advantage to have an extremely fast component. This property may be used in PET systems based on time-of-flight (TOF) tomography. When the two annihilation photons are not emitted in the center of the two detectors they might be localized due to a slight time difference in detection. As the velocity of the photons is c, the decay time of the scintillator material must be extremely fast to achieve a good resolution (a coincident time window of $500ps$ corresponds $7cm$ uncertainty in positioning). So even with CsF or BaF_2 direct positioning is not precise and reconstruction algorithms have to be used to improve the results. Nevertheless the fast response of the crystals can be used to stretch the time window for coincidences and hence eliminate random coincidences.

6.2 The photomultiplier

Photomultipliers convert light into a measurable electric current. The first element is a cathode made of photosensitive material. An incident photon here causes an electron to be emitted by the photo electric effect. Next an electron collecting system focuses the electrons. An electron multiplier system (dynode string) follows and finally the anode from which the signal will be taken. Because of a high voltage between cathode and anode the electrons are directed and accelerated toward the first dynode. This causes secondary electrons to be emitted. All these electrons are now accelerated toward the second dynode where more electrons are emitted. Along the dynode string an electron cascade is produced. At the anode these electrons give a current that can be amplified and analyzed. An ideal photomultiplier is a linear instrument. We will now have a closer look at the elements of a photomultiplier:

- **The photocathode** The photocathode converts the incident photons into electrons by the photoelectric effect. The quantum efficiency, $\eta(\lambda)$, indicates how effective this process is:

  $$\eta(\lambda) = \frac{number\ of\ photoelectrons\ released}{number\ of\ incident\ photons\ on\ cathode(\lambda)}$$

  As we can see from Einstein's formula,

  $$E = h\nu - \phi$$

  where E is the kinetic energy of the emitted photon, ν the frequency of the incident light and ϕ the work function, a minimum energy of the incident photon is necessary to make the photo electric effect possible. Above this value the probability for the photo electric effect varies with the frequency of the incident light and depends on the structure of the photosensitive

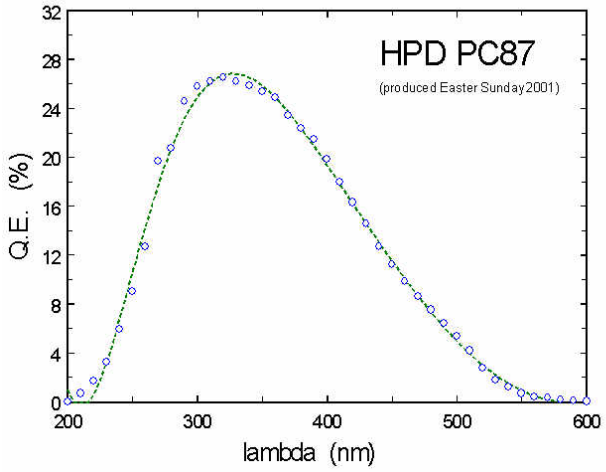

Figure 6.2: Quantum efficiency of a bialkali cathode n function of the wavelength of the incoming light [11]

material. Most photocathodes are made of semiconductor materials formed from antimony plus one ore more alkali metals. The quantum efficiency reaches a peak for a certain wavelength that should be chosen according to the wavelength of the scintillator photons. The wavelength of the peak of the alkali / bialkali cathodes is near 400 nm and the quantum efficiency there in the order of 20%. The following table shows some cathode types and their characteristics:

Cathode type	Composition	λ at peak response $[nm]$	Quantum efficiency at peak
Super A	$SbCs$	440	22
S20 (T)	$SbNa - KCs$	420	20
Bialkali D	$Sb - K - Cs$	400	26

Table 6.2: Different cathode types

The connection between the photocathode and the electron-multiplier-section is the electron-optical input system. Here the electrons are collected and focused onto the first dynode.

- **The Electron-Multiplier-Section**
  In the electron-multiplier-section the weak incident current of photoelectrons is amplified and transformed into a measurable electric current. The

section consists of a series of dynodes, usually between 10 and 14 made of a material that allows secondary electrons to escape. From one dynode to the next one, the voltage grows, the electrons gain energy and a cascade of secondary electrons is produced. The total gain reaches up to 10^7. This total gain depends on the number of dynode stages and the secondary emission factor δ - the gain at each dynode - which is a function of the material of the dynode and the energy of the incident electron and will depend on the voltage between the single dynodes

$$\delta = KV_d$$

with K a constant and V_d the potential difference between two dynodes. The total gain is then

$$G = \delta^n = (KV_d)^n$$

when n is the number of stages. A simple calculation shows, that the gain stability depends strongly on the voltage stability so that a well regulated voltage supply is of great importance. This is commonly reached by a stabilized high voltage supply together with a voltage divider consisting of a chain of resistances.

6.3 Coupling between scintillator and photomultiplier

It is of course desirable that the maximum possible amount of the light produced in the scintillator reaches the photomultiplier. Therefore it is important, to avoid the escape of photons at sides of the scintillator that are not coupled to the photomultiplier and to achieve an efficient coupling between the two elements.
The loss of light can also occur within the scintillator material through attenuation effects but since a typical attenuation length is of order $1m$ and the light intensity as a function of the traveled path is

$$L(x) = L_0 exp\left(\frac{-x}{l}\right)$$

with l the attenuation length, L_0 the incident light intensity and x the path length traveled by the light, this effect is negligible for small detectors. Light that reaches the wall of the scintillator at angles less than the Brewster angle is partially transmitted. The most common method to avoid the loss of these photons is to redirect them into the scintillator by external or internal reflectors. As such a reflector for example simple aluminum foil has been found to be quite satisfactory.
The coupling between the scintillator and the photomultiplier should allow as many photons as possible to be transmitted. For organic scintillators the optical

contact between the two media is often made by silicone grease or oil as its index of refraction is close to that of the organic material and therefore the transmission is very high. Another possibility is the transmission by light guides for example when a direct coupling is not desirable (for example because of the presence of magnetic fields) or the shape of the scintillator doesn't match with the shape of the photomultiplier.

6.4 The coincidence system

The output of the photomultiplier is an electric pulse, which should be transformed into a countable signal. In this case we are interested in counting signals proceeding from the annihilation of a positron and therefore we have two characteristics that a counted signal should fulfill: its energy is well defined (due to the $511keV$ energy of the annihilation photons) and two events must be detected simultaneously.
To achieve this goal, first we filter the signal proceeding from the photomultiplier by a discriminator, discriminating too low or too high pulses caused by noise. The coincidence system that follows will then only give a signal when two pulses coincide in time. [12][13]

Chapter 7

Positron Emission Tomography - Line-of-Response - Positioning of the detectors - Resolution

7.1 Positron Emission Tomography

Positron Emission Tomography is based on the principle of annihilation coincidence detection (ACD). The emitted positron annihilates with an electron into two photons, having both an energy of $511keV$ and the same momentum travelling in opposite directions. In this chapter we assume that the positron annihilates where it is created and the angle between the two photons is 180^o. Effects of the distance travelled by the positron before annihilation (its range) and deviations from the 180^o angle will be neglected in this chapter. The simultaneous detection of the two photons at opposite sides defines a line along which the annihilation must have taken place. This line is called the line-of-response (LOR). One pair of detectors measures all the coincidences proceeding from a certain line, it measures a line integral through the distribution. If all possible line integrals through a given plane are measured, the distribution of the activity in this plane can be reconstructed using techniques explained in chapter 9.

7.2 Line-of-Response

After the annihilation process, two photons are detected simultaneously. The line that joins the two detectors is called line-of-response. The number of coincidence events detected in a fixed time is - in the ideal case - proportional to the integral of the tracer concentration along the LOR. Of course this line has a certain volume, which primarily depends on the size of the scintillator crystal. The crystals cannot be too small as the 511 keV γ-ray should interact inside in order to be detected. But with the growing size also the error in the LOR grows.

An additional problem is the so-called depth of interaction (DOI). Before its detection, a photon might pass through one or more detectors. The detector that finally counts the photon then gives an erroneous LOR, illustrated in fig. 7.1. The effect grows with the distance to the centre. If it was possible, to measure the depth of interaction in the crystal this error could be corrected for. Attempts to estimate the DOI are a field of research.

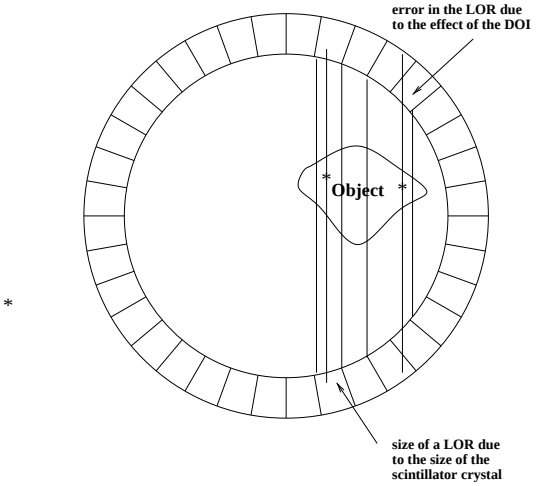

Figure 7.1: LOR - Effects of crystal size and DOI

7.3 Resolution

In general the resolution of an imaging technique is the capacity of a system to separate two small and close objects from each other. As PET is a three dimensional technique, we have to define three types of spatial resolution: axial, radial and tangential. Usually an ideal point without dimension, after the reconstruction will have a Gaussian profile. While in many imaging systems this profile is independent of its location in the image, this is not the case in PET.

At first we will have a look at the tangential and radial resolution. These two resolutions are calculated in the image plane measuring the FWHM (Full Width Half Maximum) of the radial and tangential Gaussian profile. While the FWHM of the tangential profile will be practically constant the FWHM of the radial profile will - as we have seen in the paragraph above - show a dependency on its location in the image (radial elongation).

The third resolution is the axial one or the "width of a slice". In general in

PET we try to have slices continuous, which means that the width of a slice coincides with the distance between two slices. Ultimately the tendency goes towards an isotropic voxel, so that in the final reconstructed image the resolution in direction of the three spatial axes is equal. The final resolution of a PET tomograph depends on various factors like the number and the size of the detectors, the material, the geometric position of the detectors and the reconstruction process. The final position resolution is about $5mm$ (for a BGO-crystal).

7.4 Positioning of the detectors

A PET camera usually consists of a ring of detectors placed around the object to be imaged with each of the detectors in coincidence with all the other detectors. In order to obtain a volumetric image multiple planes of rings are stacked up. For $2D$-PET imaging these planes are separated by septa, for $3D$-PET these septa are removed. Another possibility for positioning the detectors is to have two planes on opposite sides being rotated around the object. Parallel plane PET is used mostly in research and for analyzing animals, in clinical practice the ring detectors dominate. [14][15][16]

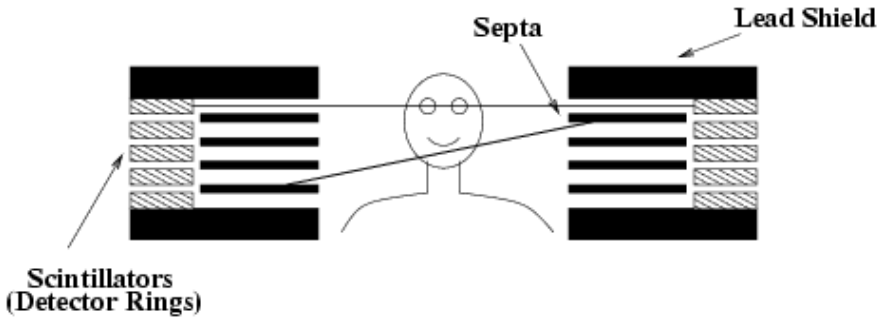

Figure 7.2: Detector rings in axial direction. For 3D adquisition the septa are removed

Chapter 8

Sinograms

In the following chapters we will have a short look at how we sample the data and transform them into a final image. As we have seen in the previous chapter, for each LOR we obtain a number of total counts. There are two possibilities to store the data. The first one is called a histogram. During the PET scan we have an individual array for each LOR. An individual storage element is called a bin and the value of a bin represents the total number of events along the corresponding LOR. The second method stores the information in list-type format. Primarily each event is stored with its corresponding LOR and at the end data are put into histograms. In $2D$-PET the histogram method dominates but in $3D$-PET where the number of LORs can get quite high and the counts for each LOR smaller than one, the list-type format often results more compact for data acquisition.

The LORs themselves are stored in so-called sinograms. As there is a difference between sinograms of $2D$- and $3D$- PET imaging we will consider them separately and begin with the less complicated $2D$-PET sinograms.

$2D$-PET Sinogram

The sinogram samples all the possible LORs in the detector ring in a two-dimensional format. Let's take the case of a ring with N_D detector elements. We imagine a coordinate system in the ring with axes x, y (see fig. 8.1). To draw the sinogram we consider all possible parallel LORs in a new coordinate system with the same origin and axes y_r parallel to the LORs and x_r perpendicular. The angle between x and x_r is named ϕ. In the sinogram we represent each LOR with its corresponding values of x_r and ϕ. We do this for angles $0 \leq \phi \leq \pi$ as the LORs repeat themselves for $\pi \leq \phi \leq 2\pi$ and the number of angular samples N_ϕ is equal to the number of detectors N_D. The number of transversal samples N_{x_r} is limited to $N_D/2$, but depending on the ratio of the scanner and the field-of-view diameters is typically limited to about the half. The name "sinogram" might be

understood considering one point within the FOV which in a sinogram traces out a sine wave.

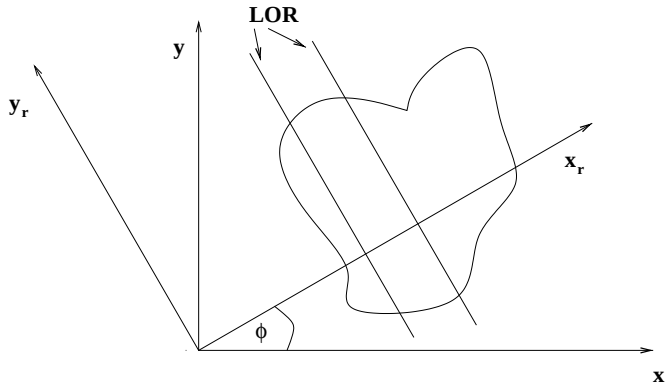

Figure 8.1: In a sinogram the LORs are represented by their values of ϕ and x_r

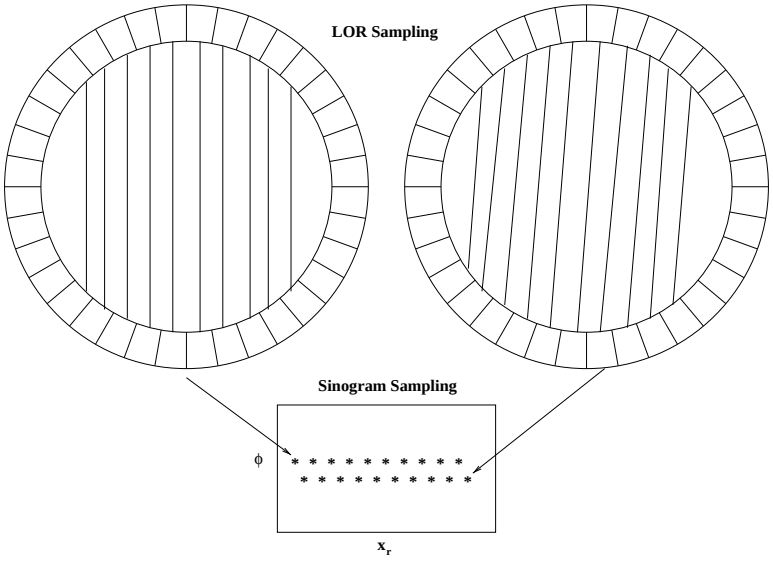

Figure 8.2: In the sinogram each LOR is represented by a point with coordinates ϕ and x_r

$3D$-PET Sinogram

In the $3D$-PET the data sampling results a bit more complicated. Instead of one ring of detectors we now have N_R rings of detectors in axial direction. Each detector ring can form a two-dimensional plane (as in $2D$-PET) with all the other

rings, so that the number of LORs is multiplied by a factor N_R^2. To describe one LOR we now need 4 coordinates (e.g. x_r, y_r, ϕ, θ). There are two formats to store the data collected in $3D$-PET, the projection format, which keeps a fixed value for (θ, ϕ) and the oblique sinogram format, which keeps fixed one value for (y_r, θ). Due to the large size of a full $3D$-PET data set, the analysis of the sampling in all 4 coordinates is very complex, so that the data are reduced by different mechanisms. [14][15]

Chapter 9

Reconstruction of images

9.1 Projection, Backprojection and Filtered Backprojection

The concern of this chapter is the reconstruction of the initial object out of the values of the line-integrals along the LORs we have sampled. The methods will be discussed for the $2D$-acquisition. In order to understand the procedures better, we will make a parallel discussion of the reconstruction of the object and a very simple case, a matrix with only one value in the centre.

Projection

Matrix

The matrix we will try to reconstruct will be a 5×5-matrix with value 1 in the centre and 0 in all the other elements:

$$\begin{matrix} 0 & 0 & 0 & 0 & 0 \\ 0 & 0 & 0 & 0 & 0 \\ 0 & 0 & 1 & 0 & 0 \\ 0 & 0 & 0 & 0 & 0 \\ 0 & 0 & 0 & 0 & 0 \end{matrix}$$

We will make a projection of this matrix in two directions. The value of the projection is the sum of all the entries of a particular line or row:

horizontal projection: vertical projection:

$$\begin{matrix} 0 \\ 0 \\ 1 \\ 0 \\ 0 \end{matrix} \qquad\qquad \begin{matrix} 0 & 0 & 1 & 0 & 0 \end{matrix}$$

PET-object

In this case, the object is described by a function $f(x, y)$ which represents the activity distribution. Projections are also made in different directions and are the line-integrals parallel to a given direction. Thus a projection drawn for a fixed value of the angle ϕ is a two-dimensional graph reflecting the value of the line-integral of a certain LOR as a function of its position x_r. The projection data are described by

$$p(x_r, \phi) = \int_{-\infty}^{\infty} dy_r f(x, y)$$

Backprojection

The aim is, to reconstruct out of the projection data (these are the data we measure in case of the PET-system) the original object. This procedure is called backprojection.

Matrix

For the matrix we can make the backprojection from two directions. As we don't know, from which element in the original matrix a certain value in the projection proceeds, we will - in a first step - backproject the value to each element of the proceeding line or row adding 1 to each of the elements in the row or column where the projection is found.

horizontal backprojection:

0	0	1	0	0
0	0	1	0	0
0	0	1	0	0
0	0	1	0	0
0	0	1	0	0

vertical backprojection:

0	0	0	0	0
0	0	0	0	0
1	1	1	1	1
0	0	0	0	0
0	0	0	0	0

The sum of the two backprojections is already very similar to the original matrix. As in the projection step we have built the sum of the elements of one row or column and in the backprojection we add this sum to each element of the corresponding row or column we have too many values in the backprojected matrix.

Backprojected matrix:

$$\begin{matrix} 0 & 0 & 1 & 0 & 0 \\ 0 & 0 & 1 & 0 & 0 \\ 1 & 1 & 2 & 1 & 1 \\ 0 & 0 & 1 & 0 & 0 \\ 0 & 0 & 1 & 0 & 0 \end{matrix}$$

PET-object

In general we can imagine the backprojection of the PET-object in a similar way to the backprojection of our matrix. The PET-object can be seen as a two- dimensional matrix with a huge number of elements (voxels). The back-propagation is done for each value of x_r at a fixed angle, incrementing the values of certain voxels. This procedure is then repeated for different angles. With this method we will receive an idea of the distribution of the activity in the object but as in the example with our matrix we will have oversampling.

Filtered backprojection

Matrix

How could we correct our backprojected matrix in order to come back to the original one? We will have to filter the values we have counted too many times. In this simple example this could be done by subtracting the following matrix:

$$\begin{matrix} 0 & 0 & 1 & 0 & 0 \\ 0 & 0 & 1 & 0 & 0 \\ 1 & 1 & 1 & 1 & 1 \\ 0 & 0 & 1 & 0 & 0 \\ 0 & 0 & 1 & 0 & 0 \end{matrix}$$

PET-object

To find a filter for the backprojection of our PET-object is of course a bit more complicated and we will have to start with some preliminary explanations.

The central section theorem

We will start with the 1D Fourier transform of the projection data. We keep the angle ϕ and transform the x_r coordinates into frequency space receiving ν_{x_r} coordinates:

$$F_1\{p(x_r, \phi)\} = P(\nu_{x_r}, \phi)$$

As a second step we will transform the object distribution data $f(x, y)$, making a 2D Fourier transform into frequency space:

$$F_2\{f(x,y)\} = F(\nu_x, \nu_y)$$

The central section theorem now tells us, that the 1D Fourier transform of the projection at an angle ϕ i s equivalent to the value along a line through the origin (at angle ϕ) of the 2D Fourier transform of f(x,y), or in formula:

$$P(\nu_{x_r}) = F(\nu_x, \nu_y)|_{\nu_{y_r}=0}$$

So one possible way of backprojection of the data is to build up a reconstruction matrix of the 1D Fourier transforms of the projection data. And at this point we find our filter: in frequency space we would have over sampling at the origin, but looking at the equation that transforms rectangular into polar coordinates $d\nu_x d\nu_y = \nu d\nu d\phi$ we see, that we will have to multiply the 1D Fourier transform (in polar coordinates) of the projection data by a factor ν in order to obtain the 2D Fourier transform (in rectangular coordinates) of the original activity distribution of the object. We have found a very simple way to filter the projection data in frequency space.

An algorithm for filtered backprojection could now for example look like this:

- Fourier transform the projection for given ϕ
- Filter the projection in frequency space (multiplication with ν)
- Inverse Fourier transform the filtered projection
- Backproject the filtered projection
- Repeat the steps for all $\phi : 0 \leq \phi < \pi$

Above a certain frequency, the spectrum is dominated by statistical noise. The application of the ramp filter (the multiplication with ν would even amplify this noise and result in a degrading signal to noise ratio. To avoid this problem a frequency low pass, correcting for high frequencies is used. The most common function used in PET is the generalized Hamming window,

$$W_H(\nu_{xr}) = \begin{cases} \alpha + (1-\alpha)\cos\left(\frac{\pi\nu_{xr}}{\nu_c}\right) & |\nu_{xr}| < \nu_c \\ 0 & |\nu_{xr}| > \nu_c \end{cases}$$

where α $(0.5 \leq \alpha \leq 1.0)$ controls the shape of the window and ν_c controls the maximum frequency.

3cm

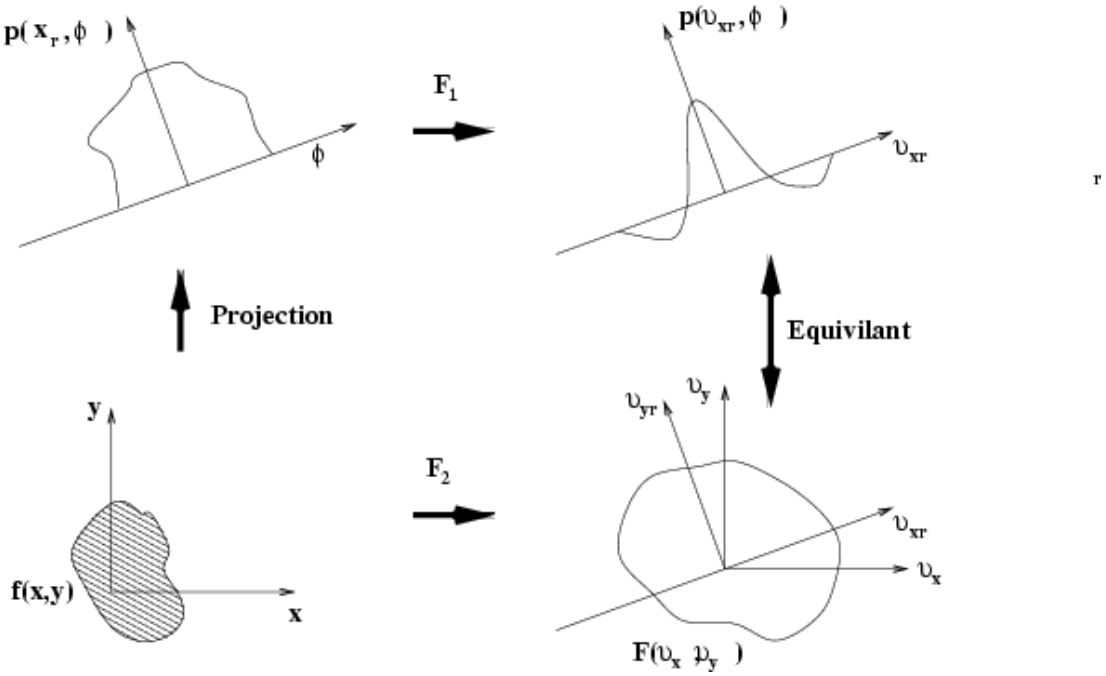

Figure 9.1: Illustration of the central section theorem

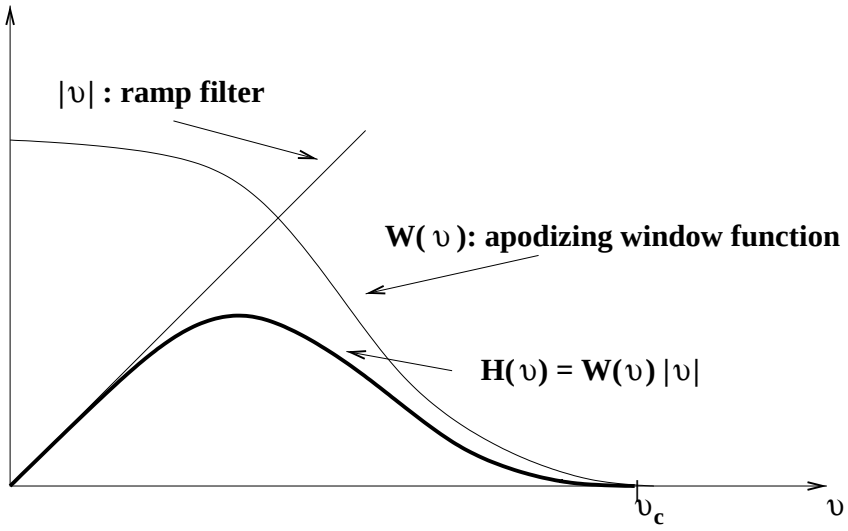

Figure 9.2: Modification of the ramp filter by multiplication with a Hamming window

9.2 Iterative Methods

In recent years, new reconstruction methods have been developed. These methods consider the Poisson statistics of the emission of positrons. The reconstruction

of the image is handled as a standard statistical problem of estimation out of incomplete data. The given data consist of a vector that contains each LOR with its number of coincidences. The original object is distributed in pixels, each pixel having a certain - unknown - activity. The method that is used, is called Expectation Maximisation (EM). It starts with a given activity distribution and calculates the probability of observing the measured data. This probability can be maximized (maximum likelihood estimation) for certain parameters describing the original distribution. This new information can be used to modify the activity distribution. This iterative method requires about 30 to 60 steps to achieve good results.

An advantage with respect to filtered backprojection is, that the statistical nature of positron emission is included in the calculation. Also corrections for other errors can be included directly, like for example corrections for attenuation, scatter, random coincidences, the range of the positron or information about the time-of-flight. An important disadvantage is the slow conversion to acceptable images and the therefore high computational costs. [14][15]

Chapter 10

Attenuation, Acolinearity, accidental coincidences

10.1 Attenuation

Figure 10.1: The probability of detecting both photons doesn't depend on the values of x_1 and x_2

Although biological tissue is almost transparent to $511keV$ photons, the probability of suffering an interaction is not negligible. γ-rays interact with matter in two different ways. Through Compton-effect, where the γ-ray looses energy and changes its direction or through the photo electric effect which means a complete absorption of the photon and therefore a loss of the coincidence. The probability of the detection of a photon in one detector is proportional to the exponential function of the line integral of the attenuation coefficient along its way to the detector:

$$n^o coincidences(det1) = \alpha_1 exp\left(-\int_{x_1} \mu(x)dx\right)$$

As measuring a coincidence means the detection of two photons, the final probability is the product of the probabilities of detecting photon 1 and photon 2.

$$n^o coincidences = \alpha_1\alpha_2 exp\left(-\int_{x_1+x_2} \mu(x)dx\right)$$

The last equation shows, that the probability for detecting an annihilation event remains constant along a certain LOR, and depends only on the distribution of matter along this line.

Until now, in order to measure the coefficients $\mu(x)$ the only method has been by use of an external source of γ-rays with an energy close to $511keV$. Before introducing the tracer the coefficient is measured in various lines through the object. Recently have been appearing combined PET-CT systems where instead of using an external source, the coefficients are estimated by the results of the CT X-rays.

10.2 Accidental coincidences

Coincidence detection is based on simultaneous detection of two photons that proceed from the same annihilation event. As the photons have a finite velocity (about $3,3ns/m$), depending on the point of annihilation there might be a slight time difference in the arrival of the two photons at the detectors. Therefore it is necessary that the coincidence can be detected although both detections don't happen simultaneously. We also have to consider, that the detection electronics have a time of response also in the region of ns. To solve this problem, a so called "coincidence window" is used. Once one photon is detected, the other detectors open a time window. If another photon is detected during this time, a coincidence event is counted and the corresponding angle and distance from the center of the line are introduced in the sinogram.

A problem occurs when during this time another photon - proceeding from another anihilation - is detected. This causes an erroneous LOR to be uptaken in the sinogram and can be considered as noise. The number of accidental coincidences can be calculated as follows:

$$coin_{ac}/s = 2\tau S_1 S_2$$

where τ is the time during which the coincidence window is open and S_1, S_2 are the numbers of single events in each detector per second. The equation shows, that with increasing activity also the number of accidental events increases possibly becoming even greater than the number of real coincidences. Knowing the number of single events in the detectors these erroneous events can be corrected for.

10.3 Acolinearity

In theory the positron and the electron have kinetic energy and momentum 0 at the time of annihilation and therefore the two annihilation-photons have each

the repose energy of an electron and they are emitted in an angle of 180^o. In praxis the electron-positron-pair has kinetic energy and momentum but very small compared to its mass energy. Due to the conservation laws this results in small deviations of the 180^o angle. To estimate this angle, we will suppose the electron-positron pair to have a momentum perpendicular to the line that combines the momenta of the two photons and the photons to have the same momentum:

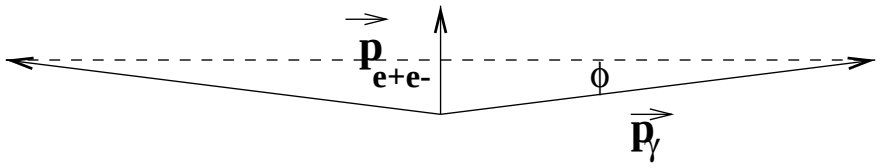

Figure 10.2: Acolinear annihilation

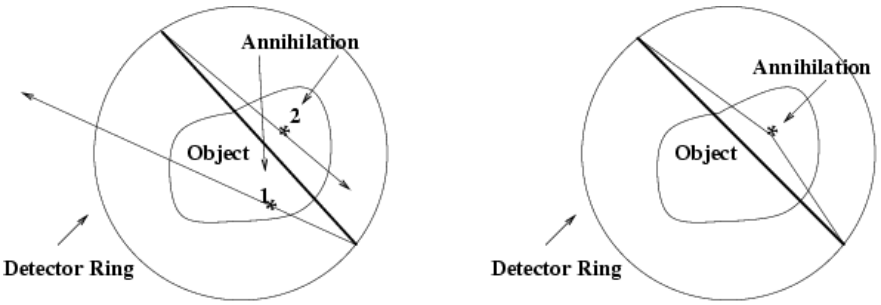

Figure 10.3: On the left: Erroneous LOR due to accidental coincidence. One photon from annihilation 1 passes through the detector and one photon from annihilation 2 is attenuated. The two remaining photons are detected in coincidence. On the right: Erroneous LOR due to acolinearity

$$
\begin{aligned}
sin(\phi) &= \frac{p_{e^+e^-}/2}{p_\gamma} \\
p_\gamma = \frac{E_\gamma}{c} = \frac{m_e c^2}{c} = m_e c \qquad & p_{e^+e^-} = (m_{e^+} + m_{e^-}) v_{e^+e^-} = 2 m_e v_{e^+e^-} \\
sin(\phi) &= \frac{(2 m_e v_{e^+e^-})/2}{m_e c} \\
&= \frac{v_{e^+e^-}}{c}
\end{aligned}
$$

A typical velocity for the electron-positron system is about $v = 10^5 \frac{m}{s}$. The error in the positioning of the point of annihilation can therefore be estimated as follows:

$$\begin{aligned} \frac{x}{d/2} &= tan(\phi) \\ &\simeq sin(\phi) \\ &= \frac{v_{e^+e^-}}{c} \\ x &\simeq \frac{v_{e^+e^-}}{c}\frac{d}{2} \\ &= 0,1mm \end{aligned}$$

x is the error in positioning, d the diameter of the detector ring estimated to 60 cm. The error x is far smaller than the resolutions obtained at the moment and therefore negligible. In future generations of detectors it could become a limiting factor for resolution. [16]

Chapter 11

Corrections of scatter

As we have seen in the previous chapter, the γ-ray on its way to the detector may suffer an interaction with matter. Instead of disappearing completely (by photo electric effect) it may also suffer a Compton scatter. In this case the γ-ray suffers an energy loss and is scattered into a new direction. As the photon keeps its property to arrive at the detector simultaneously with the other photon created in the annihilation, it causes an erroneous LOR. These erroneous data have a negative effect on the resolution of the system appearing as exponential tails added to the Gaussian resolution curves that reach zones far from its creation.

A possibility to correct for the scattered photons might be to impose an energy window in the detector. As all the γ-rays we want to detect have the same energy of 511 keV but the scattered γs have lower energy we might simply not count photons below a certain energy level. In practice this is only possible if the energy resolution of the detection system is good enough. We will now calculate the energy of the scattered γ-ray in function of the scattering angle and compare it to the energy resolutions of some of the scintillator crystals in use. Conservation of energy and momentum and the use of relativistic dynamics (necessary because of the high γ-energy) gives:

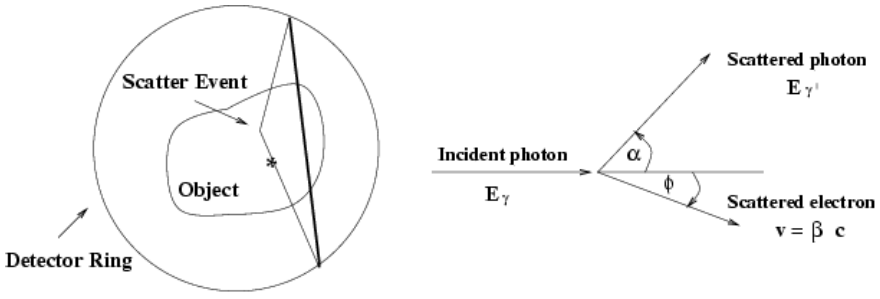

Figure 11.1: Scatter of a photon

$$\begin{aligned}
\frac{E_\gamma}{c} &= \frac{E'_\gamma}{c}\cos\alpha + \frac{mc\beta\cos\phi}{\sqrt{1-\beta^2}} \\
0 &= \frac{E'_\gamma}{c}\sin\alpha - \frac{mc\beta\sin\phi}{\sqrt{1-\beta^2}} \\
E_\gamma + mc^2 &= E'_\gamma + \frac{mc^2}{\sqrt{1-\beta^2}} \\
\Longrightarrow E'_\gamma &= \frac{E_\gamma}{1+(E_\gamma/(mc^2))(1-\cos\alpha)} \\
&= \frac{E_\gamma}{2-\cos\alpha}
\end{aligned}$$

In the last step we have used that the γ-energy is equal to the electron energy at rest.

Crystal	Energy resolution at $511keV$	Corresponding scattering angle
BGO	29%	54^o
LSO	18%	39^o
GSO	14%	33^o

Table 11.1: Energy resolution and corresponding scattering angle for commonly used scintillator crystals

All photons scattered at smaller angles could not be distinguished from the unscattered ones. The cross section for scattering at small angles is at a γ-energy of $511keV$ relatively high and therefore the method of the energy windows wouldn't be efficient with the crystals in use.

Big problems are for example points of high activity with a surrounding of very low activity. Parts of the activity of the "hot" point appears in the surrounding and is called "scattered fraction". Without corrections this would lead to errors in quantitative estimations. A possible correction method is to estimate this scatter fraction with phantoms and subtract the counts in the real image.

Another example are regions of high activity, which principally are not in the field of view of the detector. These regions must be efficiently blinded in order to not interfere in the image. [16]

Chapter 12

Trends in PET Imaging

12.1 2D $\longrightarrow$ 3D Acquisition

One trend in PET imaging goes from 2D acquisition with planes of septa placed between the detector planes to 3D acquisition where these planes are removed. The advantage is a greatly increased efficiency because many more coincidences are detected. One problem is that also noise increases but however the signal to noise ratio improves in some situations. The more complicated reconstruction is also being solved by modern computers.

12.2 New crystals

For many years BGO has been the PET crystal in use. However it is not to a perfect solution. Crystals with higher light output could improve energy resolution and shorter decay times would improve time resolution and dead time. But in order to maintain high spatial resolution the attenuation length also has to be kept small. One of the new crystals is LSO with four times higher light output, eight times faster decay time and a similar attenuation length. Another alternative is GSO with 50% higher light output and four times faster decay time but 40% longer attenuation length.

12.3 Measuring of the depth of interaction

In theory every annihilation event takes place along a line joining the two detectors that have detected the annihilation photons. A problem emerges when a photon passes through one or more detectors in the ring before it is detected. The obtained LOR is erroneous. This effect worsens when the source moves away from the center of the ring. If it was possible to measure the depth of interaction in the crystal the correct LORs could be found. So a field of research is to find

methods for estimating this depth of interaction. One solution is a detector with two different scintillator crystals in radial direction, the interaction depth can be estimated by decay time. Another possibility is to share the scintillation light between two photodetectors. The depth of interaction is determined by the ratio of light measured in each of detectors.

12.4 Special purpose PET cameras

Usual whole body PET cameras are able to image any part of the body. In order to improve imaging for only certain purposes PET cameras are optimized for example for breast cancer or small animals. As PET measures biochemical function, small animals are used to analyze the functioning of pharmaceuticals or the nature of diseases. In this case high spatial resolution is very important.

12.5 Combined PET-CT cameras

With PET we obtain functional images of biochemical procedures whereas with CT anatomical structures are revealed. In many cases a combination of the two methods could optimize the possibilities for analysis. These combined systems already exist. An x-ray CT imager and a PET imager are placed around the patient and the images are obtained without repositioning. Recently it has been shown, that the combined CT and PET image is much better at staging tumours than any of them seperately. [17]

Bibliography

[1] Steve Webb, *The Physics of Medical Imaging* Institute of Physics Publishing (1988)

[2] http://www.crump.ucla.edu/software/lpp/nuclearphyscis/lggifs/pc_10.html

[3] Joan José Pedroso de Lima, *Radiation for Health - Radioisotopes in medicine* Eur.J.Phys. 19 (1998) pp 485-497

[4] Steve Webb, *The Physics of Medical Imaging* Institute of Physics Publishing (1988) pp 181-193

[5] http://www.crump.ucla.edu/software/lpp/clinpetneuro/lggifs/restbrain.html

[6] http://www.crump.ucla.edu/software/lpp/clinpetneuro/lggifs/n_petbrainfunc_1.html

[7] http://fam-pape.de/raw/ralph/studium/teilchenphysik

[8] K.S. Krane, *Introductory Nuclear Physics* Jhon Wiley & Sons (1988) pp 198-202

[9] E. Segr=è, *Nuclei and Particles* The Benjamin/Cummings Publishing Company, Inc. (1977) pp 74-77

[10] K.S. Krane, *Introductory Nuclear Physics* Jhon Wiley & Sons (1988) pp 272-292

[11] http://ssd-rd.web.cern.ch/ssd-rd/PAD_HPD/Measurements/pad_HPD_measurements.htm

[12] W.R. Leo, *Techniques for Nuclear and Particle Physics Experiments* Springer Verlag (1994) pp 157-204

[13] M. Ribagorda, *Tomógrafos de Emisión de Positrones. Presente y Futuro de la Industria* Rev.R.Acad.Cienc.Exact.Fis.Nat.(Esp) Vol.96 N. 1-2 (2002) pp 71-75

[14] B. Bendriem, D.W. Townsend, *The Theory and Practice of 3D Pet* Kluwer Academic Publishers (1998) pp 11-30

[15] G. Kontaxakis, J.J. Vaquero, A. Santos, *Reconstrucción de Imagen en Tomografía por Emisión de Positrones* Rev.R.Acad.Cienc.Exact.Fis.Nat.(Esp) Vol.96 N. 1-2 (2002) pp 45-57

[16] J.J. Vaquero López, *Aspectos Técnicos de la Tomografía por Emisión de Positrones* Rev.R.Acad.Cienc.Exact.Fis.Nat.(Esp) Vol.96 N. 1-2 (2002) pp 3-11

[17] W.W. Moses, *Trends in PET Imaging* Nuclear Instruments and Methods in Physics Research A 471 (2001) pp 209-214